

## RESEARCH ARTICLE

# Gain-switched watt-level thulium-doped fiber laser and amplifier operating at 1.7 $\mu\text{m}$

Yang Xiao<sup>1,2</sup>, Xusheng Xiao<sup>1,2</sup>, Lutao Liu<sup>1,2</sup>, and Haitao Guo<sup>1,2</sup>

<sup>1</sup>State Key Laboratory of Transient Optics and Photonics, Xi'an Institute of Optics and Precision Mechanics, Chinese Academy of Sciences, Xi'an, China

<sup>2</sup>Center for Materials Science and Optoelectronics Engineering, University of Chinese Academy of Sciences, Beijing, China

(Received 13 August 2022; revised 21 October 2022; accepted 27 October 2022)

## Abstract

A 1.7  $\mu\text{m}$  gain-switched thulium-doped all-fiber laser with a master oscillator power amplifier (MOPA) configuration, utilizing a bandpass fiber filter and a 1550 nm erbium/ytterbium-codoped fiber MOPA, is demonstrated. The influences of pump pulse parameters (repetition rate and pulse duration) and laser cavity structures (ring and linear) on the laser performances were experimentally investigated. To the best of our knowledge, the power quenching and drop were observed in the 1.7  $\mu\text{m}$  gain-switched thulium-doped fiber lasers for the first time, resulting from the mode-locked-resembling operation and nonlinear effects. Moreover, the fiber ring-cavity laser was more stable than the linear-cavity laser in the time domain and power. Finally, a laser with a maximum average power of 1.687 W, a slope efficiency of 19.7%, a single-pulse energy of 16.87  $\mu\text{J}$ , a pulse width of 425 ns, a repetition rate of 100 kHz and a peak power of 39.69 W was obtained.

**Keywords:** 1.7  $\mu\text{m}$ ; gain-switching; fiber laser; power roll-off; thulium doping

## 1. Introduction

The strong C-H bond absorption and moderate water absorption at approximately 1.7  $\mu\text{m}$  make this wavelength band of great interest for wide applications, including methane gas detection<sup>[1]</sup>, polymer welding<sup>[2]</sup>, atmospheric sensing<sup>[3]</sup> and laser surgery<sup>[4]</sup>. In particular, 1.7  $\mu\text{m}$  short-pulsed (microsecond- or nanosecond-level pulse width) lasers with high pulse energies and high average powers are used for optical coherence tomography<sup>[5]</sup>, spectroscopic photoacoustic imaging<sup>[6]</sup> and pump sources for dysprosium-doped fiber lasers operating at approximately 4.3  $\mu\text{m}$ <sup>[7]</sup>.

To date, 1.7  $\mu\text{m}$  short-pulsed lasers have been obtained using three approaches: fiber optical parametric oscillators, Raman fiber lasers and directly pumped thulium-doped (or thulium/holmium-codoped) fiber lasers. However, 1.7  $\mu\text{m}$  short-pulsed fiber optical parametric oscillators with complex configurations tend to require specially designed high-nonlinear fibers, which compromise the performance

of the laser systems<sup>[8]</sup>. On the one hand, 1.7  $\mu\text{m}$  short-pulsed Raman solid-core fiber lasers are limited by virtue of complexity, primarily because of the high-power 1.12  $\mu\text{m}$  pump and cascaded cavity with a specially designed Raman filter fiber and multiple fiber Bragg gratings<sup>[9]</sup>. Although 1.7  $\mu\text{m}$  Raman fiber lasers pumped by 1.5  $\mu\text{m}$  erbium-doped fiber lasers can overcome such drawbacks, hundreds of meters of Raman fiber are still needed to provide sufficient Raman gain<sup>[10]</sup>. On the other hand, 1.7  $\mu\text{m}$  short-pulsed Raman fiber gas lasers utilizing hydrogen-filled hollow-core photonic crystal fibers (HC-PCFs) are expensive and involve complex and time-consuming preparation processes<sup>[11,12]</sup>, and they have relatively high fusion splice loss between the HC-PCF and solid-core fiber, which decreases the total conversion efficiency. Besides, hydrogen molecules are sufficiently small to easily penetrate the fiber cladding and overflow, thereby affecting the long-term stability of the laser. Thulium-doped silica fibers that emit an ultrabroadband luminescence across the 1.65–2.2  $\mu\text{m}$  region may open up another novel approach for approximately 1.7  $\mu\text{m}$  lasing. Admittedly, it is practically difficult to realize 1.7  $\mu\text{m}$  oscillations owing to gain saturation and strong reabsorption in thulium-doped fibers. However, several

Correspondence to: H. Guo and X. Xiao, State Key Laboratory of Transient Optics and Photonics, Xi'an Institute of Optics and Precision Mechanics, Chinese Academy of Sciences, Xi'an 710119, China. Email: guoht\_001@opt.ac.cn (H. Guo); xiaoxusheng@opt.ac.cn (X. Xiao)

exciting advancements have been made recently by exploiting various techniques to obtain 1.7  $\mu\text{m}$  continuous-wave (CW) lasers<sup>[13–27]</sup>. Despite these demonstrations, 1.7  $\mu\text{m}$  short-pulsed thulium-doped fiber lasers have not yet been fully exploited.

Generally, short-pulsed lasers can be achieved using the *Q*-switching and gain-switching techniques. However, the *Q*-switching technique has not been successfully used to obtain 1.7  $\mu\text{m}$  short-pulsed generations in thulium-doped fiber lasers due to a lack of suitable saturable absorbers. In comparison, the gain-switching technique has distinct advantages. Firstly, there is no need for an intracavity modulator, which makes the laser compact and independent from the wavelength dependence of the modulators. Secondly, it is easier to scale the output power or energy, which is usually limited by the damage threshold of the saturable absorber for passive *Q*-switching. Thirdly, the output characteristics can be flexibly controlled by tuning the pump parameters. To date, only a few studies on 1.7  $\mu\text{m}$  gain-switched thulium-doped fiber lasers have been demonstrated. Du *et al.*<sup>[28]</sup> demonstrated a compact 1.7  $\mu\text{m}$  pulsed thulium and holmium-codoped fiber laser based on a novel intermode-beating modulation technique. Li *et al.*<sup>[6]</sup> demonstrated a gain-switched thulium-doped fiber linear-cavity laser using an electrically driven acousto-optical tunable filter and a pulsed erbium-doped fiber master oscillator power amplifier (MOPA). A maximum output power of 654 mW was achieved at 1724 nm, corresponding to a pulse energy of 2.18  $\mu\text{J}$  at a repetition rate of 300 kHz. In 2020, Li *et al.*<sup>[29]</sup> achieved a 1.7  $\mu\text{m}$  laser with a maximum output power of 668 mW, a single-pulse energy of 66.8  $\mu\text{J}$  and a repetition rate of 10 kHz. However, multiple spikes in the waveform occurred and caused an unstable operation. He *et al.*<sup>[30]</sup> demonstrated a gain-switched 1728-nm thulium-doped fiber ring-cavity laser with a maximum average power of 17 mW and a single-pulse energy of 247 nJ. Recently, they achieved a thulium/holmium-codoped fiber laser by careful adjustments of the polarization controller and pump power<sup>[31]</sup>. Despite such demonstrations, the energy, average power and peak power of 1.7  $\mu\text{m}$  gain-switched thulium-doped fiber lasers remain low. In addition, those short-pulsed lasers were unstable at high pump powers. Therefore, there is strong motivation to develop high-performance gain-switched thulium-doped all-fiber lasers operating at 1.7  $\mu\text{m}$ .

In this paper, we demonstrate a 1.7  $\mu\text{m}$  short-pulsed thulium-doped all-fiber MOPA. The seed laser was a gain-switched ring-cavity thulium-doped all-fiber laser utilizing a fiber filter and a 1550 nm erbium/ytterbium-codoped fiber MOPA generating h-shaped pulses. A 1.7  $\mu\text{m}$  thulium-doped all-fiber linear-cavity laser was also fabricated. The power characteristics of the 1.7  $\mu\text{m}$  fiber linear-cavity and ring-cavity lasers at 1550 nm with pulse repetition rates in the range of 50–100 kHz and pulse durations in the range of 100–255 ns were studied and discussed in detail. Moreover,

the power roll-off phenomenon (power quenching or power drop) and the mode-locked-resembling pulses were observed in the thulium-doped all-fiber ring-cavity and linear-cavity lasers. The intrinsic reason for the generation of mode-locked operation resembling pulses is given. How the mode-locking limits the output power is analyzed in detail. The power, time domain and optical spectrum characteristics of the 1.7  $\mu\text{m}$  amplified pulsed laser at a repetition rate of 100 kHz were measured and analyzed.

## 2. Experimental setup

Figure 1(a) illustrates the experimental setup of the 1.7  $\mu\text{m}$  gain-switched all-fiber ring-cavity thulium-doped fiber laser pumped by a homemade 1550 nm pulsed erbium/ytterbium-codoped MOPA. The average power of the 1550 nm rectangular-shaped pulse seed laser was 531 mW, and the repetition rate and pulse width were adjustable in the ranges of 50–100 kHz and 200–500 ns, respectively. An optical fiber isolator (ISO<sub>1</sub>) was used to prevent the backward amplified spontaneous emission (ASE) light in the amplifier from influencing the stability of the seed laser source. The pump light from two fiber-coupled 980 nm CW laser diodes and the seed laser were coupled into a 3.4-m-long erbium/ytterbium-codoped fiber by a combiner. The core and the cladding diameters of the erbium/ytterbium-codoped fiber (Nufern, SM-EYDF-10P/125-XP) are 10 and 125  $\mu\text{m}$ , respectively, and the core numerical aperture (NA) is 0.11. The 1550 nm pulsed erbium/ytterbium-codoped fiber MOPA was used as the pump for the 1.7  $\mu\text{m}$  gain-switched thulium-doped fiber laser. A second optical fiber isolator (ISO<sub>2</sub>) was used to improve the stability of the system. The thulium-doped fiber ring-cavity (Figure 1(b)) and linear-cavity (Figure 1(c)) lasers could be selected as the seed laser source.

In the fiber ring-cavity laser, the 1550 nm pulsed laser was coupled into the thulium-doped fiber through a 1550/1710 nm fusion-type wavelength-division-multiplexing (WDM<sub>1</sub>) coupler. The core and the cladding diameters of the 3-m-long thulium-doped fiber (Nufern, SM-TSF-9/125) are 9 and 125  $\mu\text{m}$ , respectively, and the core NA is 0.15. A fiber filter with a center working wavelength of 1710 nm, an insertion loss of approximately 0.2 dB and a pass width of 20 nm was used to filter out residual pump light and the long-wavelength ASE in the 1.8–2.0  $\mu\text{m}$  wavelength band. A third optical fiber isolator (ISO<sub>3</sub>) was used to ensure unidirectional propagation of the signal laser. Twenty percent of the 1.7  $\mu\text{m}$  laser was coupled out by the output coupler at a ratio of 80:20. The total length of the cavity was approximately 14.5 m. In the fiber linear-cavity laser, the WDM coupler, fiber filter and 2 m thulium-doped fiber were the same as those in the ring-cavity fiber laser. The high-reflectivity fiber Bragg grating (HR-FBG<sub>1</sub>) centered at 1706.47 nm, with a 3 dB bandwidth of 0.31 nm, has a reflectivity of over 99.9%; and the low-reflectivity fiber Bragg grating (PR-FBG<sub>2</sub>)

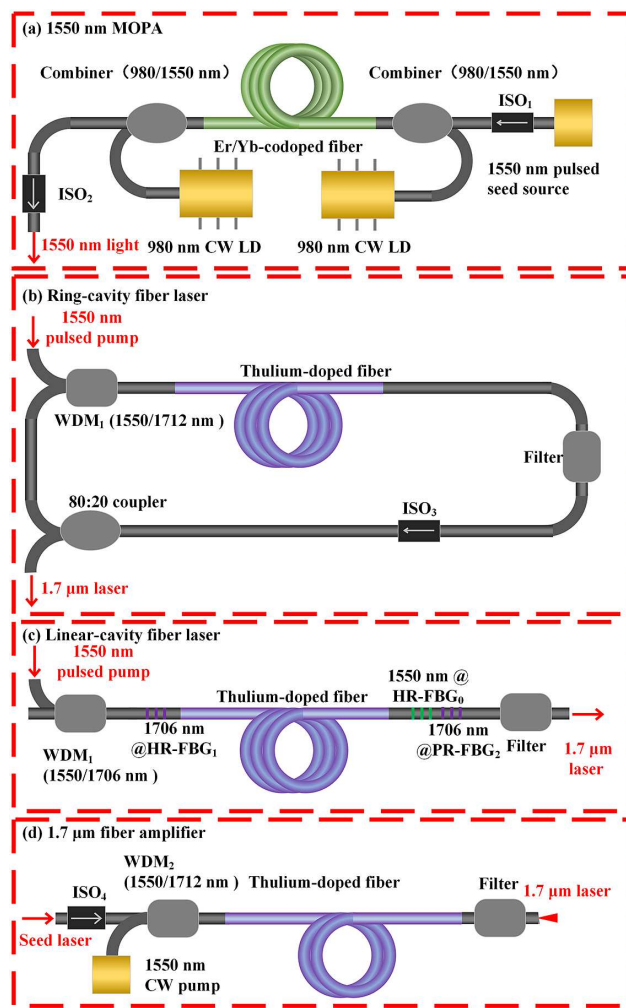


**Figure 1.** Schematic of the 1.7  $\mu\text{m}$  thulium-doped fiber MOPA pumped by a pulsed erbium/ytterbium-codoped fiber MOPA.

centered at 1706.52 nm, with a 3 dB bandwidth of 0.32 nm, has a reflectivity of approximately 31.3%. To fully absorb the pump light, a fiber Bragg grating (HR-FBG<sub>0</sub>) centered at 1550 nm with a reflectivity of over 99.9% and a linewidth of 1 nm was put between the gain fiber and FBG<sub>2</sub>. The total cavity length was approximately 8.3 m. A fourth optical fiber isolator (ISO<sub>4</sub>) was used to prevent the backward ASE light of the amplifier from influencing the stability of the 1.7  $\mu\text{m}$  seed laser source. The 1.7  $\mu\text{m}$  pulsed seed laser was injected into the thulium-doped fiber amplifier (Figure 1(d)) through a 1550/1710 nm fusion-type wavelength-division-multiplexing (WDM<sub>2</sub>) coupler. A CW 1550 nm fiber laser with a maximum power of 20 W (IPG Photonics, ELR-20-Y12) was used as the pump for the 1.7  $\mu\text{m}$  fiber amplifier and spliced with WDM<sub>2</sub>. The same type of gain fiber (2-m long) and fiber filter as those in the oscillator were used in the fiber amplifier. The fiber filter was used to filter out residual pump light and the long-wavelength ASE in the 1.8–2.0  $\mu\text{m}$  wavelength band. A thermal power meter (Thorlabs, S401C) was used to measure the power of the 1550 nm pulsed laser

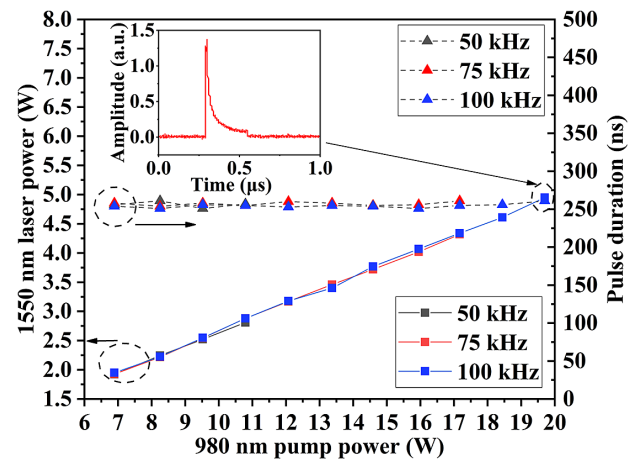


**Figure 2.** Average power and pulse duration characteristics of the 1550 nm amplified pulsed laser at repetition rates of 50, 75 and 100 kHz versus the 980 nm pump power. Inset: time domain of the 1550 nm amplified laser at a 980 nm pump power of 19.70 W and a repetition rate of 100 kHz.

from the fiber amplifier. A wavelength-insensitive thermal power meter (Ophir 12A), an optical spectrum analyzer (Yokogawa, AQ6375) with a measurement resolution of 0.05 nm and a frequency analyzer (Rohde & Schwarz) were used to measure the power, spectrum and frequency domain of the 1.7  $\mu\text{m}$  laser, respectively. The pulse train was captured by an InGaAs detector (Thorlabs, DET08CFC/M) with a band width of 5 GHz and shown on a 2-GHz bandwidth mixed-signal digital oscilloscope (Tektronix, MSO5204B).

### 3. Results

#### 3.1. The 1550 nm pulsed fiber amplifier

Figure 2 shows the power and pulse duration characteristics of the 1550 nm amplified pulsed laser at different repetition rates versus the total power of the 980 nm bi-directional pumps. When the pulse width of the 1550 nm seed laser remained at 500 ns, the variation in the average power of the 1550 nm amplified pulsed laser at the same 980 nm pump power was very small at repetition rates of 50, 75 and 100 kHz. As the power of the 980 nm pump was increased from 6.89 to 19.70 W, the power of the 1550 nm amplified laser at a repetition rate of 100 kHz increased from 1.95 to 4.95 W. The inset of Figure 2 shows the time domain of the 1550 nm pulse at a repetition rate of 100 kHz and a pump power of 19.70 W. Remarkably, the rectangular-shaped pulse became h-shaped after amplification due to the gain saturation effect<sup>[32]</sup>, which narrowed the 1550 nm pulse, and the pulse duration fluctuated at approximately 255 ns (in the range of 250–261 ns), regardless of the different repetition rates. Therefore, considering the tolerance of the error in the measurement, one could find that the pulse duration

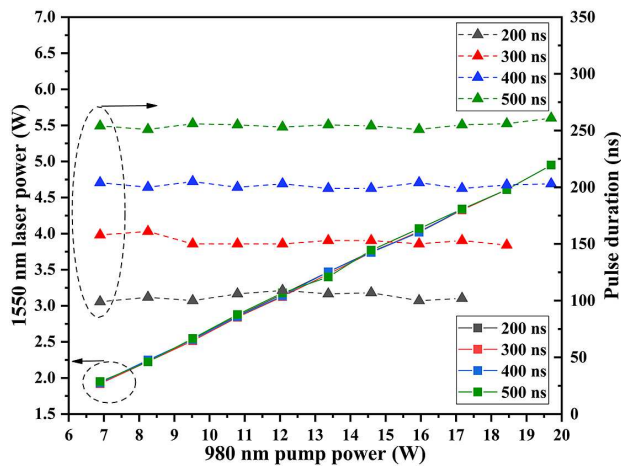


**Figure 3.** Average power and pulse duration characteristics of the 1550 nm amplified pulsed laser at seed pulse durations of 200, 300, 400 and 500 ns versus the 980 nm pump power.

remained almost unchanged. Therefore, a pulse with a higher repetition rate had a lower peak power.

Figure 3 depicts the power and pulse duration characteristics of the 1550 nm amplified pulsed laser, with the repetition rate of 100 kHz, at different seed pulse durations versus the 980 nm pump power. Note that the average powers of the 1550 nm amplified pulsed lasers at the same 980 nm pump power were almost constant at different 1550 nm seed pulse widths. Moreover, as the 980 nm pump power was increased from 6.89 to 19.70 W, the average power of the 1550 nm amplified laser at a repetition rate of 100 kHz increased from 1.95 to 4.95 W, regardless of the different seed pulse widths. The pulse durations fluctuated at approximately 100, 150, 200 and 255 ns, respectively, and were almost half of the corresponding seed pulse widths.

### 3.2. Gain-switched 1.7 $\mu\text{m}$ thulium-doped fiber ring-cavity laser

Figure 4(a) shows the power characteristics of the 1.7  $\mu\text{m}$  laser versus the power of the 1550 nm amplified pulsed laser (i.e., the pump) under the conditions of a 1550 nm amplified pulse width of 255 ns and repetition rates of 50, 75 and 100 kHz, respectively. Notably, when the pump operated at a repetition rate of 50 kHz and a power of 2.52 W, a 1.7  $\mu\text{m}$  laser with the maximum power of 0.149 W was obtained, and the laser power was quenched quickly to zero as the pump power was increased further. Actually, a pump with a lower repetition rate (a cutoff frequency) would lead to a failure of the gain-switching operation due to the limitation of the  $\text{Tm}^{3+}$  emission lifetime<sup>[33]</sup>. To the best of our knowledge, this is the first demonstration of power quenching in a 1.7  $\mu\text{m}$  gain-switched thulium-doped fiber laser. To analyze the reason for the power drop, the time domain of the 1.7  $\mu\text{m}$  laser was measured at a pump power of 2.52 W with

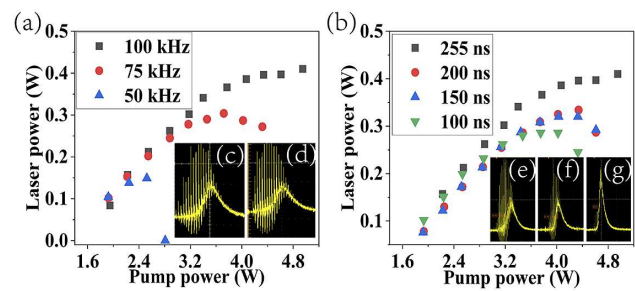


**Figure 4.** (a) Output power of the 1.7  $\mu\text{m}$  thulium-doped fiber ring-cavity laser under different pump repetition rates versus the launched pump power. Insets: (c) time domain of the 1.7  $\mu\text{m}$  laser at a pump power of 2.52 W and a repetition rate of 50 kHz; (d) time domain of the 1.7  $\mu\text{m}$  laser at a pump power of 3.72 W and a repetition rate of 75 kHz. (b) Output power of the 1.7  $\mu\text{m}$  thulium-doped fiber ring-cavity laser under different 1550 nm seed laser pulse widths versus the launched pump power. Insets: time domain of the 1.7  $\mu\text{m}$  laser at a 1550 nm amplified power (the 1550 nm amplified pulse durations and the corresponding 1550 nm seed pulse widths) of (e) 4.33 W (100 and 200 ns); (f) 4.61 W (150 and 300 ns); and (g) 4.65 W (200 and 400 ns).

a repetition rate of 50 kHz and a corresponding calculated pump pulse energy of approximately 50  $\mu\text{J}$ , as shown in the inset (c) of Figure 4(a). Evidently, these self-starting mode-locked-resembling subpulses were present within the gain-switched pulse envelope. For a more detailed analysis, the time interval between these subpulses was measured and the value was approximately 70 ns (14.3 MHz in frequency), which exactly matched the cavity round-trip time. Furthermore, in the presented mode-locked-resembling pulse trains it can be seen that the pulse durations of the subpulses were all almost 3 ns. These multiple narrow spikes only occurred on the pulse leading side and not the trailing side. This was due to the mode competition. Since more modes were coupled at the beginning of a gain-switched pulse, the intensities of the corresponding mode-locked-resembling pulses were higher, whereas few modes, due to mode competition, are coupled at the end of the gain-switched pulse. Swiderski and Michalska<sup>[34]</sup> reported a similar phenomenon in a gain-switched 1.95  $\mu\text{m}$  thulium-doped fiber laser and attributed the generation of mode-locked-resembling pulses to the beating of the laser longitudinal modes instead of the mode-locking effect because of the long pulse duration of the mode-locked-resembling pulses. The main nonlinear effect occurring when high-intensity pulses are the self-phase modulation, causes a time varying phase shift and, consequently, symmetric spectrum broadening. Once the spectrum width is comparable to or wider than the laser mode spacing, the longitudinal modes interfere, causing a periodic amplitude fluctuation at a frequency equal to the mode spacing and, consequently, mode beating. This is different from the multiple spikes described by Li *et al.*<sup>[6]</sup> and Du *et al.*<sup>[28]</sup>, in which it was attributed to the onset of mode locking induced by self-phase modulation and the polarization dependent loss of the acousto-optical tunable filter, which triggered

the nonlinear polarization rotation process. Similarly, when the pump operated at a repetition rate of 75 kHz and a power of 3.72 W, a 1.7  $\mu\text{m}$  laser with the maximum power of 0.304 W was obtained, and the laser power decreased as the pump power was increased further. At this point of inflection of the laser power, the corresponding calculated pump energy was also approximately 50  $\mu\text{J}$ . The 1.7  $\mu\text{m}$  laser power decreased to 0.272 W when the pump power was increased to 4.32 W. The time domain of the 1.7  $\mu\text{m}$  laser at a pump power of 4.32 W and a repetition rate of 75 kHz was measured, as shown in the inset (d) of Figure 4(a). There were also many self-starting mode-locked-resembling subpulses present within the gain-switched pulse envelope, which indicated that the laser power would decrease as the pump power was increased further. Furthermore, the two sets of calculated pump energies at the maximum laser power and the repetition rates of 50 and 75 kHz were almost identical, that is, approximately 50  $\mu\text{J}$ , which was the pump energy threshold for the mode-locked-resembling operation. The saturation energy for the gain-switched operation and the beating of the laser longitudinal modes may be an essential parameter. Encouragingly, the power reduction was suppressed when the pump operated at a repetition rate of 100 kHz. As the pump power was increased to 4.95 W, the maximum laser power was obtained as 0.41 W. The power characteristics at different repetition rates indicated that a high repetition rate (thus a lower pump peak power) was beneficial for the operation of the 1.7  $\mu\text{m}$  gain-switched laser. Therefore, the repetition rate was set to be 100 kHz for the stable gain-switched pulsed operation in the following section, limited by the adjustable repetition rate of the 1550 nm seed laser. Very recently, a gain-switched 1.7  $\mu\text{m}$  thulium-doped laser with a repetition rate of 134 kHz, pumped by a 1560 nm pulsed erbium/ytterbium-codoped fiber laser, was demonstrated<sup>[35]</sup>, indicating that a higher pump repetition rate was feasible for a higher laser power.

Figure 4(b) shows the power characteristics of the 1.7  $\mu\text{m}$  laser versus the pump power under different 1550 nm amplified pulse durations. When the pulse durations were 100, 150 and 200 ns, the phenomena of severe power decrease occurred at a high pump power. Inset (e)–(g) of Figure 4(b) show the time domains of the 1.7  $\mu\text{m}$  laser pulses under the conditions of 1550 nm amplified powers (1550 nm amplified pulse durations) of 4.33 W (100 ns), 4.61 W (150 ns) and 4.65 W (200 ns), respectively. Indeed, there were also mode-locked-resembling operations, which explained the phenomena of the severe power decrease. In other words, when the laser operated at the maximum output powers under the conditions of the 1550 nm amplified pulse durations of 100, 150 and 200 ns, the corresponding pump powers were 3.75, 4.03 and 4.34 W, respectively, corresponding to the pump energies of approximately 37.5, 40 and 43  $\mu\text{J}$ . As the pump powers were further increased, the mode-locked-resembling operation occurred, indicating that the pump

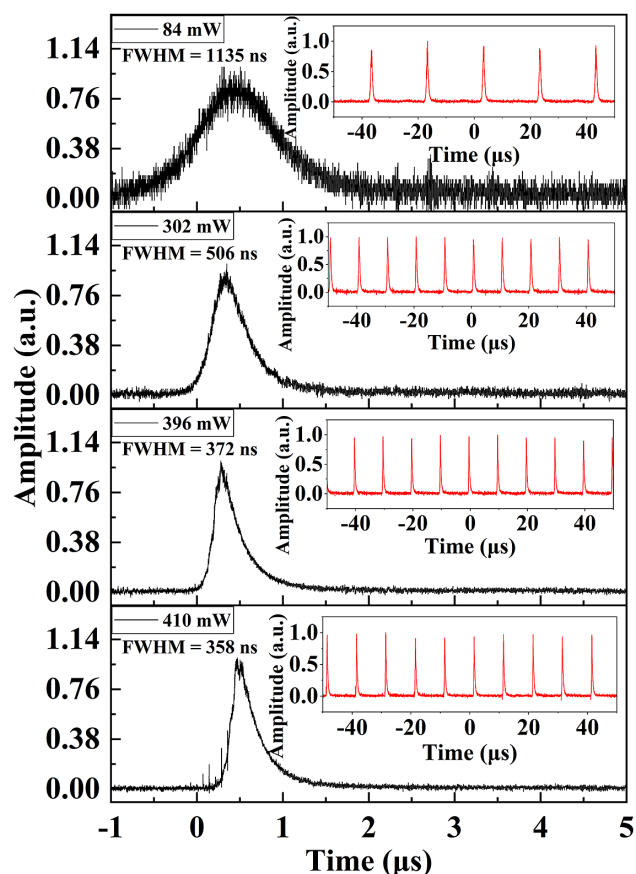


**Figure 5.** Time domain characteristics of the gain-switched 1.7  $\mu\text{m}$  thulium-doped fiber ring-cavity laser under the conditions of powers of the 1550 nm amplified lasers of 1.95, 3.18, 4.34 and 4.95 W, respectively. Insets: the corresponding pulse trains.

energy threshold for the mode-locked-resembling operation could be improved by increasing the pump pulse duration, and this further confirmed that lower pump peak power was more conducive to achieving a stable gain-switched laser operation. When the pulse duration of the 1550 nm amplified laser was 255 ns, the power decrease of the 1.7  $\mu\text{m}$  laser was suppressed to a significant extent. Therefore, limited by the adjustable pulse width of the 1550 nm seed laser, the repetition rate and the pulse duration of the 1550 nm seed laser were set to be 100 kHz and 500 ns, corresponding to an amplified pulse duration of 255 ns, respectively, for stable gain-switched pulsed operations in the following section.

Figure 5 shows the time domain characteristics of the gain-switched 1.7  $\mu\text{m}$  laser under the conditions of the pump powers of 1.95, 3.18, 4.34 and 4.95 W, respectively. The corresponding laser powers were 84, 302, 396 and 410 mW, respectively. The corresponding pulse conformations were all Gaussian lines, and the full widths at half maximum (FWHM) of the corresponding pulses were 1135, 506, 396 and 358 ns, respectively; that is, the pulse width of the 1.7  $\mu\text{m}$  laser decreased progressively as the pump power was increased. As shown in the insets, the pulse trains were

stable. As expected, there was a continuous decrease in pulse build-up time when the pump power was increased. When the pump power was 1.95 W, the pulse period was 20  $\mu\text{s}$ , corresponding to a repetition rate of 50 kHz, where the repetition rate was half that of the pump. In fact, this inversion extends well above the threshold value immediately with the next pump pulse. When the pump powers were 3.18, 4.34 and 4.95 W, the pulse periods were all 10  $\mu\text{s}$ , corresponding to a repetition rate of 100 kHz, where the repetition rate was the same as that of the pump. It is most likely that since the energy of the individual pump pulse is initially low, one pump pulse is not sufficient to generate a laser pulse; instead, it aids the population inversion in the upper laser level, and this inversion extends well above the threshold value immediately with the next pump pulse; then, when the pump energy is sufficiently high with the increased pump power, one pump pulse is sufficient to generate a laser pulse. The above temporal evolution with the pump was a typical phenomenon for gain-switching<sup>[30,36]</sup>. Notably, when the pump power and the pump pulse duration were 4.95 W and 255 ns, respectively, corresponding to the pump energy of approximately 50  $\mu\text{J}$ , there was a slight mode-locked-resembling operation, indicating that further increasing the pump power would decrease the 1.7  $\mu\text{m}$  laser power. In addition, the output pulse of the gain-switched laser exhibited slight pulse splitting, primarily because the residual pump energy was stored in the gain medium, and could drive the upper-level population above the threshold again after the emission of the first gain-switched pulse<sup>[29,30]</sup> instead of the occurrence of nonlinear phenomena, such as stimulated Brillouin scattering and stimulated Raman scattering<sup>[37]</sup>, owing to the low peak power mentioned in the following section.

Figure 6 shows the characteristics of the pulse width, peak power and single-pulse energy of the 1.7  $\mu\text{m}$  laser versus the pump power. When the pump power was 1.95 W, the repetition rate, pulse width, calculated pulse energy and peak power of the 1.7  $\mu\text{m}$  laser were 50 kHz, 1135 ns, 1.68  $\mu\text{J}$  and 1.48 W, respectively. As the pump power was increased from 2.22 W to 4.95 W, the repetition rate of the 1.7  $\mu\text{m}$  laser remained at 100 kHz, while the pulse width decreased from 901 to 358 ns. The reason for the switchable repetition rate from 50 to 100 kHz was that two pump pulses, rather than one pump pulse, were needed to produce one signal pulse until the pump power was increased to 2.22 W. We observed that the pulse width decreased rapidly at first and then tended to saturate as the pump power was further increased. This phenomenon primarily resulted from increased populations accumulated on the laser upper level with the increased pump power; specifically, there was a gradual reduction in the time required for pulse establishment. Moreover, both the peak power and pulse energy also tended to saturate as well. The most striking result was that the calculated pulse energy significantly increased from 1.57 to 4.10  $\mu\text{J}$ , and the

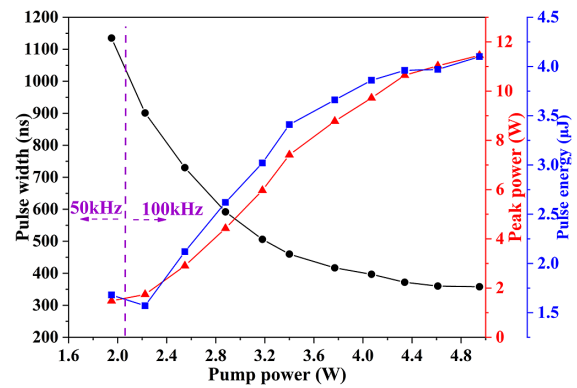


**Figure 6.** Characteristics of the pulse width, peak power and single-pulse energy of the 1.7  $\mu\text{m}$  thulium-doped fiber ring-cavity laser versus the power of the 1550 nm amplified laser.

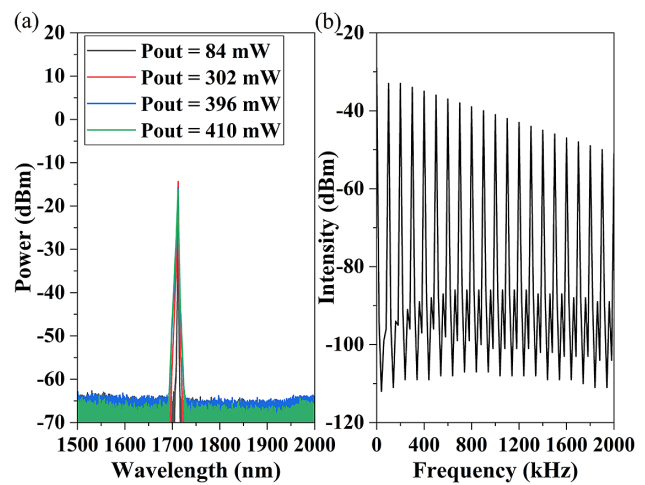


**Figure 7.** (a) Optical spectrum of the 1.7  $\mu\text{m}$  thulium-doped fiber ring-cavity laser with output powers of 84, 302, 396 and 410 mW; (b) frequency domain of the signal at a repetition rate of 100 kHz and an output power of 396 mW.

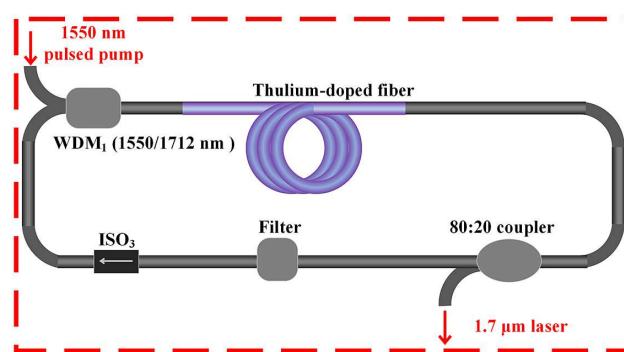
peak power increased from 1.74 to 11.45 W. To the best of our knowledge, this is the highest pulse energy and the highest average power achieved with a 1.7  $\mu\text{m}$  short-pulsed thulium-doped ring-cavity fiber laser. Although the pulse energy was much lower than that in a 1.7  $\mu\text{m}$  linear-cavity gain-switched Tm-doped fiber laser<sup>[6]</sup>, there are no strong mode-locked-resembling subpulses.

Figure 7(a) shows the optical spectrum of the 1.7  $\mu\text{m}$  laser at different laser powers. The center wavelength of the gain-switched laser was approximately 1712.3 nm. As the pump power was increased from 1.95 to 4.95 W, the 3 dB spectral width of the gain-switched laser increased from 0.35 to 1.75 nm. Such a low peak power (less than 40 W) was unlikely to enable the gain fiber to generate any nonlinear effects. Therefore, the spectrum broadening was not due to nonlinear effects. Evidently, the spectrum broadening caused by the higher number of Fourier spectral components needed for the narrowed pulses was not suppressed

because of the fiber filter having a sufficiently wide pass width<sup>[38]</sup>. The spectrum broadening may be only because of the higher number of longitudinal modes reaching the oscillation threshold when the pump power was increased. Therefore, additional longitudinal modes were contained in a laser pulse and more energy was loaded by a laser pulse, and higher power could be obtained. The outcome indicated that a fiber filter was another influential factor in the power scaling of the 1.7  $\mu\text{m}$  laser, and this explained why the maximum average and peak powers of this proposed fiber laser utilizing a bandpass fiber filter were much higher than those of the fiber laser utilizing a fiber Bragg grating with a narrow width mentioned by He *et al.*<sup>[30]</sup>. Clearly, the 1550 nm pump light was completely filtered. Besides, there was no ASE in the 1.8–2.0  $\mu\text{m}$  wavelength band. An optical signal-to-noise ratio (SNR) of approximately 50 dB could be maintained. Figure 7(b) shows the frequency spectrum of the 1.7  $\mu\text{m}$  laser with a power of 396 mW. The fundamental frequency was 100 kHz. The SNR was up to 50 dB, and the high-order amplitude exhibited a smooth drop, indicating that the single-pulse gain-switched operation was stable.

However, the intrinsic reason for the fiber laser tuning from the gain-switching regime to the mode-locking regime remains unknown and the power quenching or drop needs to be further discussed by numerical modeling of the pump modulation<sup>[33]</sup>. At a low pump power, the laser operated at the gain-switching regime; and it operated at the mode-locking regime when the pump power was high at the conditions of low pump repetition rate and narrow pump pulse duration. Intuitively, the gain saturation was relative to the mode-locked-resembling pulse operation because mode-locked-resembling pulses occurred while laser powers saturated. The growing gains with the further increasing pump power facilitate the generation of the mode-locked-resembling pulses. Seen from the insets of Figure 4, mode-locked-resembling subpulses were located at the rising edge of a gain pulse, which indicated that the mode-locked-resembling operation was earlier than the gain-switched pulse operation. Mode-locked-resembling pulses first consumed pump energy and had higher gain and, then, the gain-switched pulse consumed the rest of the pump energy. Therefore, the two lasing operations were competing. The increasing pump power caused a more serious mode-locking-resembling operation and, consequently, the power drop-off and quenching occurred.

To observe whether there were any nonlinear effects in the 1550 nm pump or thulium-doped fiber affecting the mode-locking-resembling and gain-switched pulse operations of the thulium-doped fiber ring-cavity laser, we adjust the position of the coupler behind the bandpass fiber filter, as shown in Figure 8. The output optical spectrum at a 1550 nm pump repetition rate of 100 kHz and a pulse duration of 255 ns is shown in Figure 9. The 1550 nm pump light occurred with some nonlinear effects. The highest intensity



**Figure 8.** Schematic of the thulium-doped fiber ring-cavity laser pumped at 1550 nm.

of the optical spectrum is the emission of the 1.7  $\mu\text{m}$  laser. Surprisingly, when the pump power was increased to 3.40 W, a supercontinuum (SC) spectrum between 1.7 and 2.4  $\mu\text{m}$  was generated. Its intensity got stronger with the increase of pump power. Therefore, there were nonlinear effects including stimulated Raman scattering, self-phase modulation, four-wave mixing, modulation instability, cross-phase modulation and Raman soliton self-frequency shift, which were all necessary for the generation of the SC<sup>[39]</sup>. Such nonlinear effects would influence the power scaling of the gain-switched laser. As a matter of fact, the peak power of the gain-switched 1.7  $\mu\text{m}$  output laser was a magnitude of 10 W and the gain-switched laser was thus unlikely to enable any nonlinear effect. It was the mode-locked-resembling pulses that led to the nonlinear effects and SC in the gain fiber. Obviously, the actual mode-locked-resembling pulses were strong in amplitude, although there were gain-switched pulses in the gain fiber. The self-phase modulation caused a time varying phase shift and, consequently, symmetric spectrum broadening, as shown in Figures 9 and 6(a)<sup>[34]</sup>. Note that the four-wave mixing happened in the 1550 nm pump. In addition, the emissions at 1.28 and 1.41  $\mu\text{m}$  were the diffraction harmonic light and the emissions of thulium ions, respectively. The inset of Figure 9 shows the corresponding time domain of the light from the fiber coupler at a pump power of 4.95 W. There were more mode-locked-resembling subpulses with higher intensity than those at a pump power (laser power) of 4.95 W (410 mW) in Figure 5. By comparing such subpulses with those in Figure 5, one could find out that the intensities of such subpulses were stronger and subpulses were greater in quantity. These results indicated that the fiber filter of the previous ring-cavity laser shown in Figure 1(b) actually suppresses the mode-locked-resembling pulse operation, nonlinear effects and SC generation.

To observe the power quenching, we measured the output optical spectrum at a 1550 nm pump repetition rate of 50 kHz and a pulse duration of 255 ns, as shown in Figure 10. An SC was observed, too. When the pump power was increased to 2.52 W, the 1.7  $\mu\text{m}$  laser disappeared

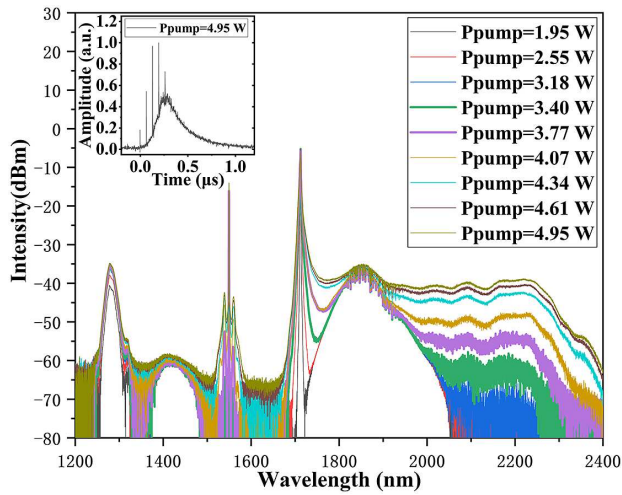


**Figure 9.** Optical spectrum of the thulium-doped fiber ring-cavity laser versus the pump power at a pump repetition rate of 100 kHz and a pump pulse duration of 255 ns.

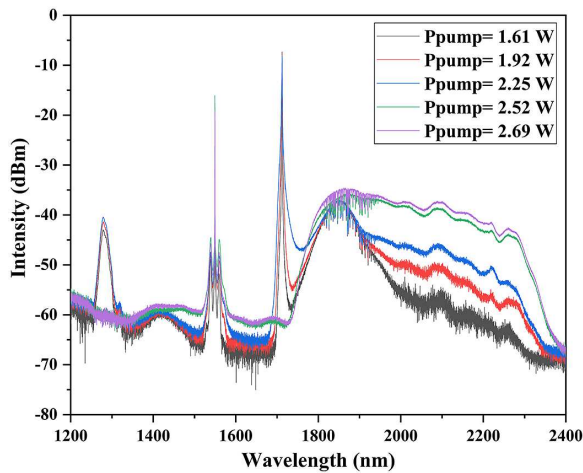


**Figure 10.** Optical spectrum of the thulium-doped fiber ring-cavity laser versus the pump power at a pump repetition rate of 50 kHz and a pump pulse duration of 255 ns.

and so did the 1.28  $\mu\text{m}$  light emission, namely, the power quenching occurred. Meanwhile, the SC spectrum between 1.7 and 2.3  $\mu\text{m}$  was enhanced. One could see that a lower pump repetition rate would lead to lower laser repetition rate, and mode-locked-resembling pulses with higher peak powers would lead to stronger nonlinear effects and, consequently, the stronger SC. One could also find that a narrower pump pulse duration leads to a higher pump energy and, consequently, more mode-locked-resembling subpulses with higher peak powers were generated. As a result, more energy was further used to generate a stronger SC.

### 3.3. Gain-switched 1.7 $\mu\text{m}$ thulium-doped fiber linear-cavity laser

Figure 11(a) shows the power characteristics of the 1.7  $\mu\text{m}$  fiber linear-cavity laser versus the pump power under the

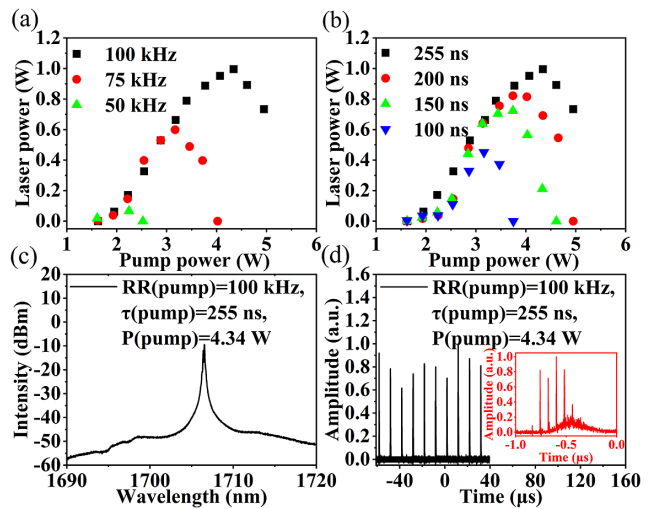


**Figure 11.** (a) Output power of the 1.7  $\mu\text{m}$  thulium-doped fiber linear-cavity laser under the conditions of a 1550 nm amplified (seed) pulse width of 255 ns (500 ns) and repetition rates of 50, 75 and 100 kHz versus the launched pump power, respectively; (b) power characteristics of the 1.7  $\mu\text{m}$  linear-cavity laser versus the pump power under 1550 nm amplified pulse durations (the corresponding 1550 nm seed pulse widths) of 100, 150, 200 and 255 ns (200, 300, 400 and 500 ns); (c) optical spectrum of the 1.7  $\mu\text{m}$  linear-cavity laser at a pump power of 4.34 W with a pump repetition rate of 100 kHz and a pump pulse width of 255 ns; (d) optical spectrum of the 1.7  $\mu\text{m}$  linear-cavity laser at a pump power of 4.34 W with a pump repetition rate of 100 kHz and a pump pulse width of 255 ns.

conditions of a 1550 nm amplified pulse width of 255 ns and repetition rates of 50, 75 and 100 kHz versus the launched pump power, respectively. When the pump operated at a repetition rate of 50 kHz and a power of 2.25 W, a 1.7  $\mu\text{m}$  laser with the maximum power of 0.067 W was obtained, and the laser power was quenched quickly to zero as the pump power was increased to 2.52 W. Likewise, at a pump power of 3.17 W, a 1.7  $\mu\text{m}$  laser with the maximum power of 0.599 W was obtained, and the laser power was quenched to zero as the pump power was increased to 4.02 W. The power quenching was also due to the strong self-starting mode-locked-resembling operation at a high pump power, shown in Figure 11(d), which was the same as that of the 1.7  $\mu\text{m}$  fiber ring-cavity laser. The power roll-off still existed when the pump operated at a repetition rate of 100 kHz. As the pump power was increased to 4.34 W, the maximum laser power was obtained as 996 mW. It should be mentioned that the laser power was very unstable and varied in several or tens of milliwatt. The power characteristics at different repetition rates indicated that a high repetition rate (thus a lower pump peak power) was beneficial for the operation of the 1.7  $\mu\text{m}$  gain-switched thulium-doped fiber laser. Therefore, the repetition rate was set to be 100 kHz for the stable gain-switched pulsed operation. Figure 11(b) shows the power characteristics of the 1.7  $\mu\text{m}$  fiber linear-cavity laser versus the pump power under different 1550 nm amplified pulse durations. When the pulse durations were 100, 150, 200 and 255 ns, the phenomenon of severe power

drop-off still occurred at a high pump power. Figure 11(c) shows the optical spectrum of the 1.7  $\mu\text{m}$  linear-cavity laser at a pump power of 4.34 W with a pump repetition rate of 100 kHz and a pump pulse width of 255 ns. The center wavelength of the laser was approximately 1706.5 nm and the 3 dB bandwidth was 0.08 nm, due to the low overlap of the bandwidths of FBG<sub>1</sub> and FBG<sub>2</sub>. Figure 11(d) shows the time domain characteristics of the gain-switched 1.7  $\mu\text{m}$  linear-cavity laser at a pump power of 4.34 W with a pump repetition rate of 100 kHz and a pump pulse width of 255 ns. The corresponding laser power was 996 mW. It should be mentioned that the time profile and train were very unstable. The mode-locked-resembling operation also occurred. The time interval between these subpulses was measured to be approximately 80 ns (12.46 MHz in frequency), which exactly matched the cavity round-trip time. The pulse durations of the subpulses were all almost 1 ns. It was believed that the mode-locked-resembling operation was due to the beating of the laser longitudinal modes<sup>[34]</sup>. The quite chaotic temporal characteristics showed unstable relaxation spike pulses with serious amplitude fluctuations that were related to mode-hopping and mode competition<sup>[40]</sup>. It could be seen that the pulse period was 10  $\mu\text{s}$ , corresponding to a repetition rate of 100 kHz. The calculated pulse energy was 9.96  $\mu\text{J}$ . Therefore, the fiber linear-cavity laser was unsuitable to seed the fiber amplifier, considering that the linear-cavity fiber laser was very unstable in the power and time domain.

Different from the linear cavity, the absence of the spatial hole-burning effect in the ring cavity facilitates the laser operation with densely spaced longitudinal modes. In addition, the spatial hole-burning effect could lead to mode coupling and further mode beating<sup>[41]</sup>. In contrast, the low overlap of the bandwidths of FBG<sub>1</sub> and FBG<sub>2</sub> in the linear cavity resulted in fewer longitudinal modes. The fewer the longitudinal modes, the easier the formation of the beating of laser longitudinal modes and the higher the peak powers of the mode-locked-resembling pulses<sup>[41]</sup>. Therefore, it is easier to generate nonlinear effects. All of these caused the unstable laser operation. Consequently, the ring cavity performed better than the linear cavity in the operation of the 1.7  $\mu\text{m}$  gain-switched thulium-doped fiber laser.

### 3.4. Pulsed 1.7 $\mu\text{m}$ thulium-doped fiber amplifier

The gain-switched 1.7  $\mu\text{m}$  thulium-doped fiber ring-cavity laser was used as the seed source. Figure 12(a) shows the power characteristics of the 1.7  $\mu\text{m}$  amplified pulsed laser at different seed powers. The repetition rate of the seed laser was 100 kHz. When the power of the 1550 nm CW pump was zero and the seed laser power was successively 0.15, 0.24 and 0.30 W, the 1.7  $\mu\text{m}$  laser was reabsorbed by the thulium-doped fiber and the output power was successively 0.005, 0.024 and 0.058 W, respectively. As the pump power was increased, the laser powers increased almost linearly

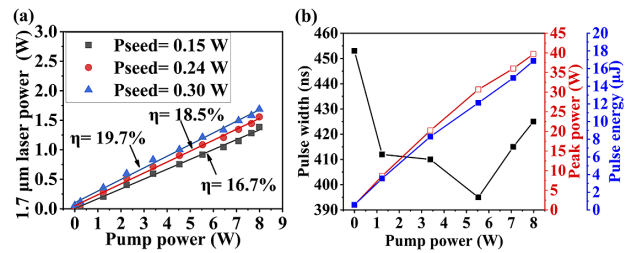


**Figure 12.** (a) Power characteristics of the 1.7  $\mu\text{m}$  amplified pulsed laser at different seed powers versus the pump power. (b) Characteristics of the pulse width, peak power and single-pulse energy of the 1.7  $\mu\text{m}$  amplified pulsed laser versus the pump power.

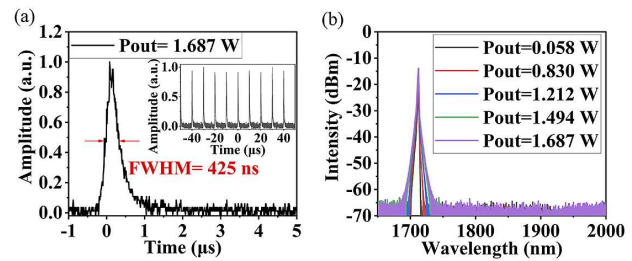


**Figure 13.** (a) Time domain characteristics of the 1.7  $\mu\text{m}$  amplified pulsed laser under the pump power of 7.99 W. (b) Optical spectrum of the 1.7  $\mu\text{m}$  amplified pulsed laser.

without any power saturation or roll-off. The corresponding calculated slope efficiencies ( $\eta$ ) were 16.7%, 18.5% and 19.7%, respectively. At the maximum pump power of 7.99 W, the maximum average powers of the 1.7  $\mu\text{m}$  laser were 1.385, 1.557 and 1.687 W, respectively. Compared with the thulium-doped fiber ring-cavity laser, the thulium-doped fiber amplifier exhibited a higher slope efficiency and a stronger power scaling capability, which indicated that a thulium-doped fiber amplifier is an effective technique for power scaling of a 1.7  $\mu\text{m}$  laser. Figure 12(b) shows the characteristics of the pulse width, peak power and single-pulse energy of the 1.7  $\mu\text{m}$  amplified pulsed laser versus the pump power. When the pump power was increased from zero to 5.53 W, the pulse width decreased from 453 to 395 ns. Then, the pulse width increased to 425 ns as the pump power was increased to 7.99 W. As the pump power was increased from zero to 7.99 W, the calculated single-pulse energy and the peak power of the 1.7  $\mu\text{m}$  laser increased almost linearly from 0.58 to 16.87  $\mu\text{J}$  and from 1.28 to 39.69 W, respectively.

Figure 13(a) shows the time domain characteristics of the 1.7  $\mu\text{m}$  amplified pulsed laser under the pump power of 7.99 W. The corresponding pulse conformation was the Gaussian line, and the FWHMs of the corresponding pulses were 425 ns with a corresponding average laser power of 1.687 W. As shown in the insets, the pulse trains were stable. The pulse period was 10  $\mu\text{s}$ , corresponding to a repetition rate of 100 kHz. Figure 13(b) shows the optical spectrum of the 1.7  $\mu\text{m}$  amplified pulsed laser with output powers of 0.058, 0.830, 1.212, 1.494 and 1.687 W. The center

wavelength of the laser was approximately 1712.3 nm, which is the same as the center wavelength of the seed laser. As the pump power was increased from 1.95 to 4.95 W, the 3 dB spectral width of the laser maintained at approximately 1.1 nm. Clearly, the 1550 nm pump light was completely filtered. Besides, there was no ASE in the 1.8–2.0  $\mu\text{m}$  wavelength band. An optical SNR of approximately 50 dB could be maintained.

One should find that the power of 688 mW in Ref. [29] was actually obtained from an unstable fiber laser because of the multiple spikes. Actually, the average and peak powers of a gain-switching laser may also be relatively low because of the strong mode-locked-resembling laser. Instead, we report the stable gain-switched pulse operation. Although the peak power of the fiber laser was only tens of watts, it may still meet some of the applications mentioned in the introduction.

#### 4. Conclusion

In summary, we demonstrated a 1.7  $\mu\text{m}$  short-pulsed thulium-doped fiber MOPA. Firstly, a gain-switched 1.7  $\mu\text{m}$  thulium-doped fiber ring-cavity laser in-band pumped by a 1550 nm erbium/ytterbium-codoped fiber MOPA was compared with a gain-switched thulium-doped fiber linear-cavity laser. The former delivered the 1.7  $\mu\text{m}$  laser with a single-pulse energy of 4.10  $\mu\text{J}$ , a repetition rate of 100 kHz, a pulse width of 358 ns and a maximum average power of 410 mW. The latter was unstable, although a maximum average power of approximately 1 W was obtained. To the best of our knowledge, this is the first demonstration of power roll-offs (power quenching or drop) in 1.7  $\mu\text{m}$  gain-switched thulium-doped fiber lasers. In addition, the mode-locked-resembling pulse operation caused by the mode beating and nonlinear effects caused by the mode-locked-resembling pulses limited the power of the gain-switched lasers. Then, the thulium-doped fiber amplifier was seeded by the gain-switched thulium-doped fiber ring-cavity laser, and delivered a 1.7  $\mu\text{m}$  laser with a maximum average power of 1.687 W, a slope efficiency of 19.7%, a single-pulse energy of 16.87  $\mu\text{J}$ , a pulse width of 425 ns, a repetition rate of 100 kHz and a peak power of 39.69 W. The results indicated that a fiber amplifier is an efficient technology for a high-energy and high-power 1.7  $\mu\text{m}$  short-pulsed laser. This investigation provides a preliminary insight into 1.7  $\mu\text{m}$  gain-switched thulium-doped fiber lasers for short-pulsed generation.

#### Acknowledgments

This work was financially supported by the National Natural Science Foundation of China (62005312, 62090065, and 61935006), the Youth Innovation Promotion Association of

the Chinese Academy of Sciences (2022409) and the Key Research and Development Projects of Shaanxi Province (2022GY-423).

#### References

1. P. Chambers, E. A. D. Austin, and J. P. Dakin, *Meas. Sci. Technol.* **15**, 1629 (2004).
2. I. Mingareev, F. Weirauch, A. Olowinsky, L. Shah, P. Kadwani, and M. Richardson, *Opt. Laser Technol.* **44**, 2095 (2012).
3. C. Anselmo, J. Y. Welschinger, J. P. Cariou, A. Miffre, and P. Rairoux, *Opt. Express* **24**, 12588 (2016).
4. V. V. Alexander, K. Ke, Z. Xu, M. N. Islam, M. J. Freeman, B. Pitt, M. J. Welsh, and J. S. Orringer, *Lasers Surg. Med.* **43**, 470 (2011).
5. U. Sharma, E. W. Chang, and S. H. Yun, *Opt. Express* **16**, 19712 (2008).
6. C. Li, J. Shi, X. Gong, C. Kong, Z. Luo, L. Song, and K. K. Y. Wong, *Opt. Lett.* **43**, 5849 (2018).
7. M. R. Majewski and S. D. Jackson, *J. Lightwave Technol.* **39**, 5103 (2021).
8. C. Li, N. Chen, X. Wei, J. Kang, B. Li, S. Tan, L. Song, and K. K. Y. Wong, *Opt. Lett.* **41**, 5258 (2016).
9. A. Grimes, A. Hariharan, Y. Sun, S. Ovtar, P. Kristensen, P. G. Westergaard, S. Rako, C. Baumgarten, R. C. Stoneman, and J. W. Nicholson, *Proc. SPIE* **11260**, 112601S (2020).
10. P. Zhang, D. Wu, Q. Du, X. Li, K. Han, L. Zhang, T. Wang, and H. Jiang, *Appl. Opt.* **56**, 9742 (2017).
11. W. Huang, Z. Li, Y. Cui, Z. Zhou, and Z. Wang, *Opt. Lett.* **45**, 475 (2020).
12. W. Pei, H. Li, W. Huang, M. Wang, and Z. Wang, *Opt. Express* **29**, 33915 (2021).
13. M. Yamada, K. Senda, T. Tanaka, Y. Maeda, S. Aozasa, H. Ono, K. Ota, O. Koyama, and J. Ono, *Electron. Lett.* **49**, 1287 (2013).
14. G. Xue, B. Zhang, K. Yin, W. Yang, and J. Hou, *Opt. Express* **22**, 25976 (2014).
15. X. Cen, X. Guan, C. Yang, C. Wang, T. Tan, W. Lin, Q. Zhao, Y. Wang, C. Huang, X. Teng, Y. Sun, K. Zhou, Z. Feng, Z. Yang, and S. Xu, *IEEE Photonics Technol. Lett.* **33**, 350 (2021).
16. S. Agger and J. H. Povlsen, *Opt. Lett.* **29**, 1503 (2004).
17. J. M. O. Daniel, N. Simakov, M. Tokurakawa, M. Ibsen, and W. A. Clarkson, *Opt. Express* **23**, 18269 (2015).
18. Z. Quan, C. Gao, H. Guo, N. Wang, X. Cui, Y. Xu, B. Peng, and W. Wei, *Sci. Rep.* **5**, 12034 (2015).
19. Z. Li, Y. Jung, J. M. O. Daniel, N. Simakov, M. Tokurakawa, P. C. Shardlow, D. Jain, J. K. Sahu, A. M. Heidt, W. A. Clarkson, S. U. Alam, and D. J. Richardson, *Opt. Lett.* **41**, 2197 (2016).
20. X. Xiao, H. Guo, Z. Yan, H. Wang, Y. Xu, M. Lu, Y. Wang, and B. Peng, *Appl. Phys. B* **123**, 135 (2017).
21. M. D. Burns, P. C. Shardlow, P. Barua, T. L. Jefferson-Brain, J. K. Sahu, and W. A. Clarkson, *Opt. Lett.* **44**, 5230 (2019).
22. J. Zhang, Q. Sheng, S. Sun, C. Shi, S. Fu, W. Shi, and J. Yao, *Opt. Commun.* **457**, 124627 (2020).
23. L. Zhang, J. Zhang, Q. Sheng, S. Sun, C. Shi, S. Fu, X. Bai, Q. Fang, W. Shi, and J. Yao, *Opt. Express* **28**, 37910 (2020).
24. L. Zhang, J. Zhang, Q. Sheng, C. Shi, W. Shi, and J. Yao, *Opt. Express* **29**, 27048 (2021).
25. L. Zhang, J. Zhang, Q. Sheng, Y. Li, C. Shi, W. Shi, and J. Yao, *Opt. Express* **29**, 25280 (2021).
26. J. Zhang, Q. Sheng, L. Zhang, C. Shi, S. Sun, X. Bai, W. Shi, and J. Yao, *Opt. Express* **29**, 21409 (2021).
27. L. Zhang, J. Zhang, Q. Sheng, S. Fu, W. Shi, and J. Yao, *Opt. Laser Technol.* **152**, 108180 (2022).

28. T. Du, Q. Ruan, R. Yang, W. Li, K. Wang, and Z. Luo, *J. Lightwave Technol.* **36**, 4894 (2018).
29. C. Li, J. Shi, X. Wang, B. Wang, X. Gong, and L. Song, *Photonics Res.* **8**, 160 (2020).
30. Z. He, P. Zhang, D. Wu, X. Wu, S. He, J. Wei, X. Gong, X. Li, T. Wang, K. Han, and S. Tong, *Opt. Laser Technol.* **131**, 106450, (2020).
31. Q. Li, P. Zhang, Y. Fan, Y. Ning, J. Wei, and S. Tong, *Appl. Opt.* **61**, 455 (2022).
32. P. Grzes and J. Swiderski, *IEEE Photonics J.* **10**, 1500408 (2018).
33. Y. Wang, S. Y. Set, and S. Yamashita, in *Conference on Lasers and Electro-Optics (CLEO)* (2017), paper SM4L.4.
34. J. Swiderski and M. Michalska, *Opt. Lett.* **38**, 1624 (2013).
35. L. Zhang, J. Zhang, Q. Sheng, S. Fu, Y. Li, C. Shi, W. Shi, and J. Yao, *J. Lightwave Technol.* **40**, 4373 (2022).
36. D. Pal, A. Paul, S. D. Chowdhury, M. Pal, R. Sun, and A. Pal, *Appl. Opt.* **57**, 3546 (2018).
37. B. N. Upadhyaya, U. Chakravarty, A. Kuruvilla, K. Thyagarajan, M. R. Shenoy, and S. M. Oak, *Opt. Express* **15**, 11576 (2007).
38. H. Luo, J. Li, Y. Hai, X. Lai, and Y. Liu, *Opt. Express* **26**, 63 (2018).
39. I. Zorin, P. Gattinger, A. Ebner, and M. Brandstetter, *Opt. Express* **30**, 5222 (2022).
40. C. Wei, H. Luo, H. Shi, Y. Liu, H. Zhang, and Y. Liu, *Opt. Express* **25**, 8816 (2017).
41. P. Myslinski, J. Chrostowski, J. A. K. Koningstein, and J. R. Simpson, *Appl. Opt.* **32**, 286 (1993).